Non-rigid and tough calcium phosphate cement scaffold seeded with umbilical cord stem cell for bone repair

WahWah Thein-Han[1], Michael D. Weir[1], Carl G. Simon[2], Hockin H. K. Xu[1,3*]

[1] Biomaterials & Tissue Engineering Division
Department of Endodontics, Prosthodontics and Operative Dentistry
University of Maryland Dental School, Baltimore, MD 21201;
[2]Biomaterials Group, National Institute of Standards and Technology (NIST)
Gaithersburg, MD 20899;
[3] Center for Stem Cell Biology & Regenerative Medicine
University of Maryland School of Medicine, Baltimore, MD 21201, USA

For: *Biomaterials*
Submitted in December 2010

* Corresponding author:
Hockin Xu
Professor, Director of Biomaterials & Tissue Engineering Division
University of Maryland Dental School, 650 West Baltimore Street, Baltimore, MD 21201
Ph: 410-706-7047. Fax: 410-706-2089. E-mail: hxu@umaryland.edu

Running title: Non-rigid CPC scaffold with umbilical cord stem cells

Key Words: Calcium phosphate cement (CPC), non-rigid scaffold, human umbilical cord stem cells, osteogenic differentiation, bone tissue engineering.

Abstract

Human umbilical cord mesenchymal stem cells (hUCMSCs) are a promising alternative to bone marrow MSCs, which require invasive procedures to harvest. The objectives of this study were to develop a novel non-rigid and tough calcium phosphate cement (CPC), and to investigate hUCMSC proliferation, osteodifferentiation and mineralization on non-rigid CPC for the first time. Non-rigid CPC scaffold was fabricated using extra tetracalcium phosphate in the CPC powder, chitosan, absorbable fibers and alginate microbeads. The non-rigid CPC-microbead scaffold possessed a strain-at-failure of 10.7%, higher than conventional CPC's strain of 0.05%, which is typical for brittle bioceramics. The flexural strength of non-rigid CPC-microbead scaffold was 4-fold that of rigid CPC-mircobead scaffold. Work-of-fracture (toughness) was increased by 20-fold. The non-rigid CPC-microbead-fiber scaffold matched the strength of cancellous bone. hUCMSCs on non-rigid CPC increased from about 100 cells/mm^2 at 1 d, to 600 cells/mm^2 at 8 d. Alkaline phosphatase, osteocalcin, and collagen gene expressions of hUCMSCs were greatly increased, and the cells successfully synthesized bone minerals. hUCMSCs on non-rigid CPC-microbead-fiber construct had higher bone marker expressions and more mineralization than those on rigid CPC. Non-rigid CPC could potentially provide compliance for micro-motions within the tissues, with load-supporting strength for periodontal bone repair, spinal fusion and other repairs. In conclusion, this study developed the first non-rigid, self-setting calcium phosphate-microbead scaffold with a strain-at-failure exceeding 10%. hUCMSCs showed excellent proliferation, osteodifferentiation, and mineral synthesis on non-rigid CPC scaffolds. The hUCMSC-CPC construct with excellent cell proliferation, osteodifferentiation and mineral synthesis is promising for bone regeneration.

1. Introduction

New bone regeneration approaches are needed to repair large defects resulting from trauma, disease, and tumor resection [1,2]. In the United States, nearly seven million people suffer bone fractures each year, and musculoskeletal conditions cost $215 billion annually [3-7]. These numbers are increasing due to an aging population. To meet this need, novel scaffold and stem cell approaches are being investigated [8-15]. Human umbilical cord mesenchymal stem cells (hUCMSCs) are highly promising [16-22]. They can be harvested without the invasive procedure required for bone marrow MSCs (BMSCs). Umbilical cords are inexhaustible, and the cost is low as they are currently a medical waste. hUCMSCs appeared to be a primitive MSCs population that expressed certain human embryonic stem cell markers and exhibited a high degree of plasticity and developmental flexibility, with no immunorejection in preliminary animal studies [18].

Engineered scaffolds serve as a matrix for cell function while maintaining the volume and supporting the external stresses. Due to their similarity to apatite minerals in natural bone, calcium phosphate (CaP) bioceramics such as hydroxyapatite (HA) are important for bone repair [23,24]. CaP implants are bioactive and provide an ideal environment for cellular reaction and colonization by osteoblasts, thus forming a functional interface *in vivo* [25-27]. Previous efforts have enhanced the properties of CaP scaffolds and implants [23,28,29]. For preformed bioceramic scaffolds to fit in a bone cavity, the surgeon needs to machine the graft or carve the surgical site, leading to increases in bone loss, trauma, and surgical time [2]. In contrast, calcium phosphate cements can be injected and set in the bone cavity to provide intimate adaptation to the defects, and can be replaced by new bone [30-33]. The first calcium phosphate cement (CPC) was developed in 1986 [30]. Since then, several other formulations were developed [34-38]. CPC was approved in 1996 by the Food and Drug Administration (FDA) for repairing craniofacial defects and became the first CaP cement for clinical use [32,33]. However, due to its brittleness, CPC is "limited to the

reconstruction of non-stress-bearing bone" [31,32]. Recently, absorbable fibers and chitosan were used to improve the load-bearing capability of CPC [39-41].

It is desirable to improve CPC into a non-rigid and tough scaffold. When the traditional rigid CPC was used in periodontal bone repair, tooth mobility resulted in the early displacement and failure of the brittle implants [42]. A non-rigid CPC would be useful to provide the needed compliance for tooth motion without fracturing the implant. Chitosan and its derivatives are biodegradable and osteoconductive, and are good candidates for the elastomeric matrix [43,44]. In a recent study, a non-rigid CPC was developed by using chitosan [45], achieving a high ductility for potential applications in orthopedic and craniofacial repairs such as periodontal bone repair, alveolar bone augmentation, and spinal fusion. However, while hydrogel beads and fibers were added in the regular CPC [46], they have not been incorporated into the non-rigid CPC. In addition, stem cell seeding on non-rigid CPC is yet to be investigated.

The objectives of this study were to develop a hUCMSC-seeded, non-rigid CPC-hydrogel composite construct, and investigate the osteogenic differentiation of hUCMSCs on non-rigid CPC for the first time. It was hypothesized that: (1) While the CPC composite construct would be weak mechanically, adding chitosan and fibers would increase its strain-at-failure and strength; (2) hUCMSCs on non-rigid CPC composite would have good viability and proliferation rate; (3) Non-rigid CPC composite would support hUCMSC differentiation, and adding chitosan and fibers would enhance bone marker gene expressions and mineral synthesis by the hUCMSCs.

2. Materials and methods

2.1 Calcium phosphate powder and liquid

The CPC powder consisted of a mixture of tetracalcium phosphate (TTCP) ($Ca_4[PO_4]_2O$) and dicalcium phosphate anhydrous (DCPA) ($CaHPO_4$). TTCP was synthesized from a solid-state

reaction between equimolar amount of DCPA and calcium carbonate (J.T. Baker, Philipsburg, NJ). The mixture was heated to 1500 ºC then quenched to room temperature, ground and sieved to obtain TTCP particles of 1 to 80 μm, with a median of 17 μm [33,47]. DCPA was ground to obtain a median particle size of 1 μm. Two CPC powders were prepared. The first consisted of a mixture with a TTCP:DCPA molar ratio of 1 to 1. This ratio was the same as that of the conventional CPC [32], and it is referred to as "rigid CPC". A second powder used a TTCP:DCPA ratio of 3.7 to 1, following a previous study [45]. The higher TTCP content was shown to facilitate the gelling of chitosan, yielding a CPC-chitosan composite with a high ductility [45]. The rigid CPC used water as liquid as in previous studies [32], and served as the control. For the non-rigid CPC, a chitosan liquid was used by mixing chitosan lactate (VANSON, Redmond, WA) with water at a chitosan/(chitosan + water) mass fraction = 15%, following a previous study [45].

2.2 Calcium phosphate-hydrogel microbead composite

The non-rigid CPC of the previous study did not contain hydrogel microbeads or absorbable fibers [45]. It is desirable to include hydrogel microbeads in CPC to potentially deliver growth factors, and then for the microbeads to degrade and form macropores in CPC. The present study focused on the effect of microbeads and fibers on the mechanical properties of the non-rigid CPC, as well as the seeding of hUCMSCs for osteogenic differentiation. A future study will investigate the delivery of various growth factors in the microbeads in CPC. To make microbeads, a sodium alginate solution (1.2% mass fraction) was prepared by dissolving 0.3 g alginate (ProNova, Oslo, Norway) in 25 mL of 155 mM sodium chloride [46]. The alginate solution was sprayed from a syringe into a 100 mM calcium chloride solution, where gelation occurred upon contact. The syringe was connected to a bead generation device (Nisco, Zurich, Switzerland) [46]. Nitrogen gas at a pressure of 10 psi was fed to the gas inlet to form a coaxial air flow with which to break up the

alginate into fine droplets. The microbeads thus fabricated had diameters ranged from 73 to 465 μm (mean = 207 μm), suitable for injection delivery and macropore formation in CPC [46].

Three groups of specimens were made. Group 1 had two materials: Rigid CPC-microbead scaffold which served as control; and non-rigid CPC-microbead scaffold. Each CPC powder was mixed with the liquid at a powder:liquid mass ratio of 2:1 to form a paste. Hydrogel microbeads were mixed with the paste, at a microbead volume/specimen volume fraction of 50%. The paste was placed into a rectangular mold of 3 x 4 x 25 mm^3. The specimen was incubated in a humidor at 37 ºC for 4 h, then immersed in a simulated physiological solution (1.15 mmol/L Ca, 1.2 mmol/L P, 133 mmol/L NaCl, 50 mmol/L Hepes, buffered to a pH 7.4) at 37 ºC for 20 h.

The purpose of group 2 was to investigate the effect of fiber reinforcement on mechanical properties of non-rigid CPC-microbead specimens. A resorbable suture fiber (Vicryl, polyglactin 910, Ethicon, NJ) at 3 mm length was used because this fiber had a high strength, provided reinforcement for about four weeks, and then dissolved and formed macropores in CPC [39]. The fibers were mixed with the non-rigid CPC + microbead paste at fiber volume fractions of 0%, 10%, 20%, 30%, and 40%. Fibers more than 40% were not used in order to obtain a flowable CPC paste. The fiber volume fraction was equal to the volume of fibers divided by the volume of the entire specimen. Specimens were fabricated in the same manner as described for the first group.

The purpose of group 3 was to investigate hUCMSC seeding and osteogenic differentiation. Three materials were tested: Rigid CPC control; non-rigid CPC-microbead scaffold; and non-rigid CPC-microbead-fiber scaffold. The fiber volume fraction was 40%. The paste was mixed as described above and filled into a circular mold of a diameter of 11.5 mm and a thickness of 1.5 mm. The disks were sterilized in an ethylene oxide sterilizer (Andersen, Haw River, NC) for 12 h according to the manufacturer's specifications, and then degassed for 7 d prior to cell experiments.

2.3 Mechanical testing

Mechanical properties were tested via a standard three-point flexural test with a span of 20 mm at a crosshead speed of 1 mm/min on a computer-controlled Universal Testing Machine (MTS, Eden Prairie, MN). Flexural strength, work-of-fracture, elastic modulus, and strain-at-failure were measured. Work-of-fracture (toughness) is a measurement of the energy required to fracture the specimen, calculated as the area under the load-displacement curve divided by the specimen's cross-sectional area. Because the fiber-reinforced scaffolds did not break completely, a cut-off displacement of 3 mm was used to calculate the work-of-fracture [41].

2.4 hUCMSC attachment, proliferation, and viability

hUCMSCs (ScienCell Research Laboratories, Carlsbad, CA) were derived from umbilical cords of healthy babies, and harvested using methods described previously [16,19]. The use of hUCMSCs was approved by the University of Maryland at Baltimore. Cells were cultured in a low-glucose Dulbecco's modified Eagle's medium (DMEM), supplemented with 10% fetal bovine serum (FBS) and 1% penicillin-streptomycin (10,000 IU-10,000 μg/ml) (Invitrogen, Carlsbad, CA). This media is referred to as "control media". At 80-90% confluence, hUCMSCs were detached by trypsin and passaged. Passage 4 hUCMSCs were used. The osteogenic media contained 100 nM dexamethasone, 10 mM β-glycerophosphate, 0.05 mM ascorbic acid, and 10 nM 1α,25-Dihydroxyvitamin (Sigma) [21,46]. A cell suspension of 150,000 cells in 2 mL of osteogenic media was added to each well containing a scaffold disk. The media was changed every 2 d.

After 1, 4, and 8 d, the media was removed and the cell-scaffold constructs were washed in Tyrode's Hepes buffer. Cells were stained with a live/dead kit (Invitrogen), and viewed by epifluorescence microscopy (TE2000S, Nikon, Melville, NY). Three randomly-chosen fields of view were photographed from each disk. Five disks yielded 15 photos for each material at each

time point. The cells were counted. N_{Live} is the number of live cells. N_{Dead} is the number of dead cells. The percentage of live cells, $P = N_{Live}/(N_{Live} + N_{Dead})$ [47]. Live cell density, D, is the number of live cells attached to the specimen divided by the surface area, A: $D = N_{Live}/A$ [46].

hUCMSCs were seeded on the scaffolds and cultured for 1 d and 4 d. They were fixed with 2.5% glutaraldehyde in 0.1 M cacodylate buffer pH 7.4, dehydrated with a graded series of ethanol (25-100%), rinsed with hexamethyldisilazane and sputter-coated with gold. They were then examined using a scanning electron microscope (SEM, JEOL 5300, Peabody, MA).

2.5 Immunofluorescence of actin fibers in hUCMSCs attached on scaffolds

Actin stress fibers inside the cells are related to initial cell attachment. hUCMSC constructs after 1 d culture were washed with PBS, fixed with 4% parformaldehyde for 20 min, permeabilized with 0.1% Triton X-100 for 5 min, and blocked with 0.1% bovine serum albumin (BSA) for 30 min [44]. An actin cytoskeleton and focal adhesion staining kit (Chemicon, Temecula, CA) was used, which stained actin fibers into a red color. Fluorescence microscopy (TE2000S, Nikon) was used to examine the specimens. The actin fluorescence intensity was increased when there was a higher density of actins stress fibers. The fluorescence intensity of actin fibers in hUCMSCs was measured via a NIS-Elements BR software (Nikon).

2.6 hUCMSC osteogenic differentiation

Quantitative real-time reverse transcription polymerase chain reaction measurement (qRT-PCR, 7900HT, Applied Biosystems, Foster City, CA) was performed to quantify osteogenic differentiation. Each well containing a CPC disk was seeded with 150,000 cells and cultured in osteogenic media for 1, 4, and 8 d [48]. The total cellular RNA on the scaffolds were extracted with TRIzol reagent (Invitrogen) and reverse-transcribed into cDNA. TaqMan gene expression kits were

used to measure the transcript levels of the proposed genes on human alkaline phosphatase (ALP, Hs00758162_m1), Osteocalcin (OC, Hs00609452_g1), collagen type I (Coll I, Hs00164004), and glyceraldehyde 3-phosphate dehydrogenase (GAPDH, Hs99999905). Relative expression for each target gene was evaluated using the $2^{-\Delta\Delta Ct}$ method [49]. The Ct values of target genes were normalized by the Ct of the TaqMan human housekeeping gene GAPDH to obtain the ΔCt values. These values were then subtracted by the Ct value of the hUCMSCs cultured on tissue culture polystyrene in the control media for 1 day (the calibrator) to obtain the ΔΔCt values [46,48].

2.7 hUCMSC mineralization

First, hUCMSCs were seeded on tissue culture polystyrene (TCPS), and cultured in control media or osteogenic media for 14 d. Alizarin Red S (ARS) staining was used to visualize bone mineralization. The adherent cells were washed with PBS, fixed with 10% formaldehyde, and stained with ARS (Millipore, Billerica, MA) for 5 min, which stained calcium-rich deposits by cells into a red color. The purpose of this step was to determine that hUCMSCs on TCPS in osteogenic media could indeed synthesize minerals, as TCPS itself contained no minerals.

Second, hUCMSCs were seeded on rigid CPC, non-rigid CPC-microbead, and non-rigid CPC-microbead-fiber scaffolds. The cells on the disks were cultured in osteogenic media for 14 d and then stained with ARS to visualize mineralization by the hUCMSCs. In addition, an osteogenesis assay kit (Millipore, Billerica, MA) was used to extract the stained minerals and measure the Alizarin Red concentration at $OD_{405,}$ following the manufacture's instructions. Control CPC without hUCMSC seeding was also measured. The control's Alizarin Red concentration was subtracted from the Alizarin Red concentration of the corresponding scaffold with hUCMSCs, to yield the net mineral concentration synthesized by the cells.

One-way and two-way ANOVA were performed to detect significant effects of the variables. Tukey's multiple comparison tests were done to compare the data at *p* of 0.05.

3. Results

Fig. 1 shows the mechanical behavior of group 1. In (A), the rigid CPC-mircobead specimen fractured catastrophically with little deformation. In (B), the non-rigid CPC-microbead specimen was able to bend extensively without fracture. This was quantified in (C), which showed that the rigid CPC-mircobead specimens fractured at a displacement of about 0.1 mm, while the non-rigid CPC-microbead specimens reached a large displacement of 3 mm before fracture. Flexural strength in (D) of the non-rigid CPC-microbead specimens was 4-fold higher than that of rigid CPC-mircobead specimens ($p < 0.05$). Work-of-fracture in (E) was increased from 5 J/m^2 for rigid CPC-mircobead to 123 J/m^2 for non-rigid CPC-microbead ($p < 0.05$). In (F), elastic moduli were not significantly different ($p > 0.1$). In (G), the strain-at-failure for the non-rigid CPC-microbead reached 10.7%, much higher than the 0.05% of the rigid CPC-mircobead specimens ($p < 0.05$).

Mechanical properties of group 2 are plotted in Fig. 2. In (A), all specimens showed a non-catastrophic failure, with the load-bearing capability increasing with higher fiber content. In (B), the maximum flexural strength increased with fiber content, reaching (3.8 ± 1.1) MPa at 40% fibers. Work-of-fracture also significantly increased with fibers ($p < 0.05$). Elastic modulus increased but not significantly ($p > 0.1$), likely because the fibers were flexible and not stiff.

In Fig. 3, live cells were stained green and were numerous on all materials (A-C). Cells proliferated well, with many more cells at 8 d (D-F). Dead cells were stained red and were very few. The percentage of live cells (G) was above 90% for all constructs. In (H), the hUCMSC density increased from about 100 cells/mm^2 at 1 d, to nearly 600 cells/mm^2 at 8 d ($p < 0.05$). The

cell density on the non-rigid CPC-microbead-fiber scaffold increased from (125 ± 12) cell/mm^2 at 1 d, to (323 ± 96) cell/mm^2 at 4 d, and (604 ± 99) cell/mm^2 at 8 d.

The fluorescence results of actin stress fibers are shown in Fig. 4. Compared to the rigid CPC in (A), the red fluorescence intensified on (B) the non-rigid CPC-microbead, and (C) the non-rigid CPC-microbead-fiber scaffold. This indicates an increased number of actin stress fibers in the hUCMSCs. The higher magnification in (D) shows numerous actin stress fibers. In (E), the actin fiber fluorescence intensity, proportional to the amount of actin fibers, increased from rigid CPC to non-rigid CPC-microbead, and to non-rigid CPC-microbead-fiber scaffold ($p < 0.05$).

SEM micrographs of hUCMSC attachment on the scaffolds are shown in Fig. 5. In (A), after 1 d, the cells attached and spread well on rigid CPC. In (B) and (C), the cells attached to the non-rigid CPC-microbead-fiber construct. "C" refers to the hUCMSCs, with cytoplasmic extensions "E" that anchored to the fibers "F". Higher magnification in (D) showed that the cells also anchored to the nano-sized apatite crystals that made up the CPC matrix. Cells attained a normal polygonal morphology.

The osteogenic differentiation results are plotted in Fig. 6. In (A), the ALP gene expression was minimal at 1 d, greatly increased at 4 d, then slightly decreased at 8 d. At 4 d, the hUCMSCs of the non-rigid CPC-microbead-fiber construct had the highest ALP peak, followed by that of non-rigid CPC construct, and then followed by rigid CPC; these three values were significantly different from each other ($p < 0.05$). In (B), the OC gene expression peaked at 8 d. At 8 d, the OC values of non-rigid CPC-microbead-fiber and the non-rigid CPC constructs were not significantly different from each other; both were higher than that of rigid CPC ($p > 0.1$). In (C), the collagen I gene expression showed a similar trend as that of OC.

ARS stains calcium minerals into a red color. In Fig. 7A, hUCMSCs were cultured in control media, and no red staining was found. In Fig. 7B, hUCMSCs on TCPS in osteogenic media

showed significant mineral staining. In (C), ARS staining yielded a red color for the CPC disk with no cells, because CPC consisted of hydrxyapatite minerals. When hUCMSCs were seeded on (D) rigid CPC, (E) non-rigid CPC-microbead scaffold, and (F) non-rigid CPC-microbead-fiber scaffold, the red staining became progressively thicker and darker than that of CPC disk without cells. There was a layer of new mineral matrix synthesized by the cells covering the disks. The thick matrix mineralization formed in the cell-scaffold construct covered not only the top surface, but also the peripheral areas at the sides of the disk. The data from the osteogenesis assay is plotted in (G). The mineral synthesized by the hUCMSCs on the non-rigid CPC-microbead-fiber scaffold was significantly more than those of the other two constructs ($p < 0.05$).

4. Discussion

CPC bioceramic scaffolds are highly biocompatible, bioactive and osteoconductive, and hence are important for bone repairs [30-38]. However, bioceramics are brittle and typically fracture catastrophically after a small deformation strain. The present study developed the first non-rigid CPC-hydrogel microbead composite scaffold with a large strain-at-failure of 10.7%. The micribeads could potentially encapsulate cells and growth factors to enhance bone regeneration. In contrast, the rigid CPC had a strain-at-failure of only 0.05%, typical for brittle ceramics. CPC is highly promising for bone repair because it can be injected and set in the bone cavity to provide intimate adaptation to the defects. A non-rigid CPC can provide compliance for micro-motions within the tissue without fracture, and can be useful for applications such as periodontal bone repair and spinal fusion. In our previous study, a non-rigid CPC was formulated but it did not contain hydrogel microbeads or absorbable fibers [45], and there had been no study on stem cell seeding on the non-rigid CPC. In the present study, the addition of absorbable fibers increased the strength of the non-rigid CPC containing 50% by volume of alginate hydrogel microbeads. The strength of

approximately 4 MPa of the construct approached the reported tensile strength of 3.5 MPa for cancellous bone [50]. To our knowledge, this is the first non-rigid calcium phosphate cement scaffold with hydrogel microbeads that matched the strength of cancellous bone. Previous studies have developed injectable polymeric scaffolds for cell delivery. A study reported that injectable polymeric carriers for cell delivery had a compressive strength of about 0.7 MPa and modulus of 0.008 GPa [51]. Other studies reported that hygrogels had a tensile strength of about 0.07 MPa and a modulus of 0.0001 GPa [52,53]. These novel materials are meritorious for stem cell delivery in non-load-bearing applications. However, it was concluded that "Hydrogel scaffolds are used in nonload bearing bone tissue engineering. … They do not possess the mechanical strength to be used in load bearing applications" [53]. In the present study, the non-rigid CPC-microbead-fiber construct is much stronger mechanically, and may be useful for stem cell delivery in a wide range of load-bearing maxillofacial and orthopedic applications.

While hBMSCs are an important cell source for bone regeneration, their limitations include donor site morbidity, and lower self-renewal and differentiation potential with aging. Recent studies demonstrated the promise of hUCMSCs, in which cells were cultured with tissue culture plastic, polymer scaffolds, and calcium phosphate scaffolds for tissue engineering [16-22]. While hUCMSC delivery via the regular rigid CPC-based scaffold was investigated [46], the present study investigated hUCMSC seeding on the non-rigid CPC scaffold. hUCMSCs were able to adhere, spread and remain viable on the non-rigid CPC. hUCMSCs anchored to the nano-sized apatite crystals and fibers in the non-rigid scaffold. They proliferated rapidly on the scaffold, with the cell number increasing by 6-fold in 7 d. The immunofluorescence experiment showed that actin stress fibers were numerous in the hUCMSCs attaching to the CPC-based scaffolds. These actin stress fibers anchor to the cell membrane at locations that are frequently connected to the extracellular matrix or the scaffold substrate. These connection sites are called focal adhesions [44]. The

fluorescence intensity of the actin stress fibers of hUCMSCs on the non-rigid CPC-microbead-fiber scaffold was nearly 2-fold that of the rigid CPC. The non-rigid CPC contained chitosan which the rigid CPC did not have. It is possible that the chitosan and the fibers have enhanced cell attachment; further studies are needed to confirm and understand the mechanisms.

The hUCMSCs successfully differentiated into the osteogenic lineage while attaching to the non-rigid scaffold. ALP, OC, and collagen I gene expressions were shown in previous studies to play key roles in the osteogenic differentiation of MSCs [17-19,21,54-56]. The present study showed that these osteogenic markers were highly expressed by the hUCMSCs while anchoring to the non-rigid CPC. ALP is an enzyme expressed by MSCs during osteogenesis and is a well-defined marker for their differentiation [12,26,27]. Previous studies showed that the ALP gene expression was low at 1 d, peaked at 4 d, and then decreased at 8 d [48]. The OC expression showed a high peak at 8 d, which was slightly later than ALP peak at 4 d [48]. Our results for the hUCMSCs in the non-rigid CPC constructs are consistent with the previous results.

The fiber-containing construct had higher ALP at 4 d than those without fibers. The OC and collagen I expressions of hUCMSCs were also higher for the non-rigid CPC-microbead-fiber construct than those for the rigid CPC without fibers. The Vicryl suture fiber used in the non-rigid construct consisted of individual fibers braided to form a bundle. The individual fiber diameter was about 14 μm. The bundle had a diameter of about 300 μm and it had a rough surface. The rough surface of the non-rigid CPC-microbead-fiber construct likely facilitated the hUCMSC attachment and osteogenic differentiation. For example, a recent study showed a 3-fold greater bone tissue ingrowth in defects containing carbon-nanotube nanocomposite scaffold, compared to control polymer scaffolds without nanotubes [57]. The previous study attributed this large increase to the high surface area and roughness, which may have enhanced cell attachment and stimulated the cells to synthesize the extracellular matrix [57]. Furthermore, the non-rigid CPC without fibers also had

higher ALP, OC and collagen I expressions than the rigid CPC. Hence, it is possible that the incorporation of chitosan, which the rigid CPC did not contain, may have also contributed to the osteodifferentiation of the cells on the non-rigid CPC [58]. The ARS mineral staining became a darker and thicker red when the non-rigid CPC contained fibers, compared to that without fibers. The hUCMSCs of the non-rigid CPC-microbead-fiber scaffold synthesized much more bone minerals than that of the rigid CPC. These results indicate that the non-rigid CPC-microbead-fiber scaffold seeded with hUCMSCs may be a promising construct for bone tissue engineering. Further animal studies are needed to investigate its bone regeneration efficacy.

5. Conclusions

This study developed a novel non-rigid CPC-hydrogel construct, and investigated hUCMSC proliferation, osteodifferentiation and mineral synthesis on non-rigid CPC for the first time. The non-rigid calcium phosphate-hydrogel scaffold had a strain-at-failure exceeding 10%; in contrast, rigid CPC fractured at a strain of 0.05%, typical for brittle bioceramics. The non-rigid CPC could provide the needed compliance for micro-motions within the tissues and yet have load-supporting strength, with applications such as periodontal bone repair, alveolar bone augmentation, and spinal fusion. The strength of the non-rigid scaffold matched that of cancellous bone. hUCMSC density on non-rigid CPC increased by 5 fold in 7 days. hUCMSCs on the non-rigid CPC-microbead-fiber construct had higher ALP, OC and collagen I expressions than those on conventional rigid CPC. hUCMSCs synthesized much more bone mineral on the non-rigid CPC-microbead-fiber scaffold than rigid CPC. The non-rigid, high-strain CPC with excellent hUCMSC proliferation, differentiation and mineral synthesis is promising for bone tissue engineering.

Acknowledgment

We thank Dr. L. C. Chow and Dr. S. Takagi at the Paffenbarger Research Center and Dr. Liang Zhao at the University of Maryland Dental School for discussions and help. This study was supported by NIH grants R01 DE14190 and R01 DE17974 (HX), Maryland Stem Cell Research Fund grant 2008-MSCRFE-0109-00 (HX), and the University of Maryland Dental School.

References

[1] Praemer A, Furner S, Rice DP. Musculoskeletal conditions in the United States. Rosemont, Illinois: American Academy of Orthopedic Surgeons. Chapter 1, 1999.

[2] Laurencin CT, Ambrosio AMA, Borden MD, Cooper JA. Tissue engineering: orthopedic applications. Annu Rev Biomed Eng 1999;1:19-46.

[3] Sikavitsas VI, Bancroft GN, Holtorf HL, Jansen JA, Mikos AG. Mineralized matrix deposition by marrow stromal osteoblasts in 3D perfusion culture increases with increasing fluid shear forces. Proc Natl Acad Sci USA 2003;100:14683-14688.

[4] Rahaman MN, Mao JJ. Stem cell based composite tissue constructs for regenerative medicine. Biotechnol Bioeng 2005;91:261-284.

[5] Huang YC, Kaigler D, Rice KG, Krebsbach PH, Mooney DJ. Combined angiogenic and osteogenic factor delivery enhances bone marrow stromal cell-driven bone regeneration. J Bone Miner Res 2005;20:848-857.

[6] Hofmann S, Hagenmuller H, Koch AM, Müller R, Vunjak-Novakovic G, Kaplan DL, Merkle HP, Meinel L. Control of in vitro tissue-engineered bone-like structures using human mesenchymal stem cells and porous silk scaffolds. Biomaterials 2007;28:1152-1162.

[7] Mao JJ, Giannobile WV, Helms JA, Hollister SJ, Krebsbach PH, Longaker MT, Shi S. Craniofacial tissue engineering by stem cells. J Dent Res 2006;85:966-979.

[8] Lavik E, Langer R. Tissue engineering: Current state and perspectives. Applied Microbiol & Biotech 2004;65:1-8.

[9] Mauney J, Volloch V, Kaplan DL. Matrix-mediated retention of osteogenic differentiation potential by human adult bone marrow stromal cells during ex vivo expansion. Biomaterials 2004;25:3233-3243.

[10] Yao J, Radin S, Reilly G, Leboy PS, Ducheyne P. Solution-mediated effect of bioactive glass in poly (lactic-co-glycolic acid)-bioactive glass composites on osteogenesis of marrow stromal cells. J Biomed Mater Res A 2005;75:794-801.

[11] Benoit DSW, Nuttelman CR, Collins SD, Anseth KS. Synthesis and characterization of a fluvastatin-releasing hydrogel delivery system to modulate hMSC differentiation and function for bone regeneration. Biomaterials 2006;27:6102-6110.

[12] Mao JJ, Vunjak-Novakovic G, Mikos AG, Atala A. Regenerative medicine: Translational approaches and tissue engineering. Boston and London: Artech House. Chapter 6-13, 2007.

[13] Johnson PC, Mikos AG, Fisher JP, Jansen JA. Strategic Directions in Tissue Engineering. Tissue Eng 2007;13:2827-2837.

[14] Discher DE, Mooney DJ, Zandstra PW. Growth factors, matrices, and forces combine and control stem cells. Science 2009;324:1673-1677.

[15] Chatterjee K, Lin-Gibson S, Wallace WE, Parekh SH, Lee YJ, Cicerone MT, Young MF, Simon CG Jr. The effect of 3D hydrogel scaffold modulus on osteoblast differentiation and mineralization revealed by combinatorial screening. Biomaterials 2010;31:5051-5062.

[16] Wang HS, Hung SC, Peng ST. Mesenchymal stem cells in the Wharton's jelly of the human umbilical cord. Stem Cells 2004;22:1330-1337.

[17] Baksh D, Yao R, Tuan RS. Comparison of proliferative and multilineage differentiation potential of human mesenchymal stem cells derived from umbilical cord and bone marrow. Stem Cells 2007;25:1384-1392.

[18] Can A, Karahuseyinoglu S. Concise review: human umbilical cord stroma with regard to the source of fetus-derived stem cells. Stem Cells 2007;25:2886-2895.

[19] Bailey MM, Wang L, Bode CJ, Mitchell KE, Detamore MS. A comparison of human umbilical cord matrix stem cells and temporomandibular joint condylar chondrocytes for tissue engineering temporomandibular joint condylar cartilage. Tissue Eng 2007;13:2003-2010.

[20] Jäger M, Degistirici O, Knipper A, Fischer J, Sager M, Krauspe R. Bone healing and migration of cord blood-derived stem cells into a critical size femoral defect after xenotransplantation. J Bone Miner Res 2007;22:1224-1233.

[21] Wang L, Singh M, Bonewald LF, Detamore MS. Signalling strategies for osteogenic differentiation of human umbilical cord mesenchymal stromal cells for 3D bone tissue engineering. J Tissue Eng Regen Med 2009;3:398-404.

[22] Zhao L, Burguera EF, Xu HHK, Amin N, Ryou H, Arola DD. Fatigue and human umbilical cord stem cell seeding characteristics of calcium phosphate-chitosan-biodegradable fiber scaffolds. Biomaterials 2010;31:840-847.

[23] Ducheyne P, Qiu Q. Bioactive ceramics: the effect of surface reactivity on bone formation and bone cell function. Biomaterials 1999;20:2287-2303.

[24] Miranda P, Pajares A, Saiz E, Tomsia AP, Guiberteau F. Fracture modes under uniaxial compression in hydroxyapatite scaffolds fabricated by robocasting. J Biomed Mater Res A 2007;83:646-655.

[25] Foppiano S, Marshall SJ, Marshall GW, Saiz E, Tomsia AP. The influence of novel bioactive glasses on in vitro osteoblast behavior. J Biomed Mater Res A 2004;71:242-249.

[26] Leach JK, Kaigler D, Wang Z, Krebsbach PH, Mooney DJ. Coating of VEGF-releasing scaffolds with bioactive glass for angiogenesis and bone regeneration. Biomaterials 2006;27:3249-3255.

[27] Reilly GC, Radin S, Chen AT, Ducheyne P. Differential alkaline phosphatase responses of rat and human bone marrow derived mesenchymal stem cells to 45S5 bioactive glass. Biomaterials 2007;28:4091-4097.

[28] Pilliar RM, Filiaggi MJ, Wells JD, Grynpas MD, Kandel RA. Porous calcium polyphosphate scaffolds for bone substitute applications - in vitro characterization. Biomaterials 2001;22:963-972.

[29] Deville S, Saiz E, Nalla RK, Tomsia AP. Freezing as a path to build complex composites. Science 2006;311:515-518.

[30] Brown WE, Chow LC. A new calcium phosphate water setting cement. In: Brown PW, editor, Cements research progress. Westerville, OH: American Ceramic Society. p. 352-379, 1986.

[31] Shindo ML, Costantino PD, Friedman CD, Chow LC. Facial skeletal augmentation using hydroxyapatite cement. Arch Otolaryngol Head Neck Surg 1993;119:185-190.

[32] Friedman CD, Costantino PD, Takagi S, Chow LC. BoneSource hydroxyapatite cement: a novel biomaterial for craniofacial skeletal tissue engineering and reconstruction. J Biomed Mater Res B 1998;43:428-432.

[33] Chow LC. Calcium phosphate cements: Chemistry, properties, and applications. Mater Res Symp Proc 2000;599:27-37.

[34] Barralet JE, Gaunt T, Wright AJ, Gibson IR, Knowles JC. Effect of porosity reduction by compaction on compressive strength and microstructure of calcium phosphate cement. J Biomed Mater Res B 2002;63:1-9.

[35] Bohner M, Gbureck U, Barralet JE. Technological issues for the development of more efficient calcium phosphate bone cements: A critical assessment. Biomaterials 2005;26:6423-6429.

[36] Bohner M, Baroud G. Injectability of calcium phosphate pastes. Biomaterials 2005;26:1553-1563.

[37] Link DP, van den Dolder J, van den Beucken JJ, Wolke JG, Mikos AG, Jansen JA. Bone response and mechanical strength of rabbit femoral defects filled with injectable CaP cements containing TGF-β1 loaded gelatin microspheres. Biomaterials 2008;29:675-682.

[38] Xu HHK, Weir MD, Simon CG. Injectable and strong nano-apatite scaffolds for cell/growth factor delivery and bone regeneration. Dent Mater 2008;24:1212-1222.

[39] Xu HHK, Quinn JB, Takagi S, Chow LC. Synergistic reinforcement of in situ hardening calcium phosphate composite scaffold for bone tissue engineering. Biomaterials 2004;25:1029-1037.

[40] Xu HHK, Weir MD, Burguera EF, Fraser AM. Injectable and macroporous calcium phosphate cement scaffold. Biomaterials 2006;27:4279-4287.

[41] Xu HHK, Carey LE, Burguera EF. Strong, macroporous, and in situ-setting calcium phosphate cement layered structures. Biomaterials 2007;28:3786-3796.

[42] Brown GD, Mealey BL, Nummikoski PV, Bifano SL, Waldrop TC. Hydroxyapatite cement implant for regeneration of periodontal osseous defects in humans. J Periodont 1998;69:46-157.

[43] Muzzarelli RAA, Biagini G, Bellardini M, Simonelli L, Castaldini C, Fraatto G. Osteoconduction exerted by methylpyrolidinone chitosan used in dental surgery. Biomaterials 1993;14:39-43.

[44] Thein-Han WW, Shah J, Misra RD. Superior in vitro biological response and mechanical properties of an implantable nanostructured biomaterial: Nanohydroxyapatite-silicone rubber composite. Acta Biomater 2009;5:2668-2679.

[45] Xu HHK, Takagi S, Sun L, Hussain L, Chow LC, Guthrie WF, Yen JH. Calcium phosphate cement with non-rigidity and strength durability for periodontal bone repair. J Am Dent Assoc 2006;137:1131-1138.

[46] Zhao L, Weir MD, Xu HHK. An injectable calcium phosphate - alginate hydrogel - umbilical cord mesenchymal stem cell paste for bone tissue engineering. Biomaterials 2010;31:6502-6510.

[47] Moreau JL, Xu HHK. Mesenchymal stem cell proliferation and differentiation on an injectable calcium phosphate-chitosan composite scaffold. Biomaterials 2009;30:2675-2682.

[48] Kim K, Dean D, Mikos AG, Fisher JP. Effect of initial cell seeding density on early osteogenic signal expression of rat bone marrow stromal cells cultured on cross-linked poly(propylene fumarate) disks. Biomacromol 2009;10:1810-1817.

[49] Livak KJ, Schmittgen TD. Analysis of relative gene expression data using real-time quantitative PCR and the $2^{-\Delta\Delta Ct}$ Method. Methods 2001;25:402-408.

[50] Damien CJ, Parsons JR. Bone graft and bone graft substitutes: a review of current technology and applications. J Appl Biomater 1990;2:187-208.

[51] Shi X, Sitharaman B, Pham QP, Liang F, Wu K, Edward Billups W, Wilson LJ, Mikos AG. Fabrication of porous ultra-short single-walled carbon nanotube nanocomposite scaffolds for bone tissue engineering. Biomaterials 2007;28:4078-4090.

[52] Kuo CK, Ma PX. Ionically crosslinked alginate hydrogels as scaffolds for tissue engineering: part I. Structure, gelation rate and mechanical properties. Biomaterials 2001;22:511-521.

[53] Drury JL, Dennis RG, Mooney DJ. The tensile properties of alginate hydrogels. Biomaterials 2004;25:3187-3199.

[54] Datta N, Holtorf HL, Sikavitsas VI, Jansen JA, Mikos AG. Effect of bone extracellular matrix synthesized in vitro on the osteoblastic differentiation of marrow stromal cells. Biomaterials 2005;26:971-977.

[55] Lavery K, Hawley S, Swain P, Rooney R, Falb D, Alaoui-Ismaili M. New insights into BMP-7 mediated osteoblastic differentiation of primary human mesenchymal stem cells. Bone 2009;45:27-41.

[56] Zhang ZY, Teoh SH, Chong MS, Schantz JT, Fisk NM, Choolani MA, Chan J. Superior osteogenic capacity for bone tissue engineering of fetal compared with perinatal and adult mesenchymal stem cells. Stem Cells 2009;27:126-137.

[57] Sitharaman B, Shi X, Walboomers XF, Liao H, Cuijpers V, Wilson LJ, Mikos AG, Jansen JA. In vivo biocompatibility of ultra-short single-walled carbon nanotube/biodegradable polymer nanocomposites for bone tissue engineering. Bone 2008;43:362–370.

[58] Thein-Han WW, Saikhun J, Pholpramoo C, Misra RD, Kitiyanant Y. Chitosan-gelatin scaffolds for tissue engineering: physico-chemical properties and biological response of buffalo embryonic stem cells and transfectant of GFP-buffalo embryonic stem cells. Acta Biomater 2009;5:3453-3466.

Figure captions

[1] Mechanical behavior of group 1. (A) Conventional rigid CPC fractured catastrophically. (B) Non-rigid CPC-microbead scaffold showed a transition to a tough and non-catastrophic fracture mode. (C) Typical load-displacement curves. (D) Flexural strength, (E) work-of-fracture (toughness), (F) elastic modulus, and (G) strain-at-failure. Each value is the mean of five measurements with the error bar showing one standard deviation (mean ± sd; n = 5).

[2] Mechanical properties of group 2. (A) Non-catastrophic failure of the fiber-reinforced non-rigid CPC scaffold. (B) Maximum flexural strength, (C) work-of-fracture, and (D) elastic modulus, vs. fiber volume fraction. Each value is mean ± sd; n = 5.

[3] Live/dead results of hUCMSCs for group 3. (A-C) Live cells were stained green and were numerous on all materials. (D-F) hUCMSCs proliferated and increased in cell density by 8 d. (G) Percentage of live cells. (H) hUCMSCs proliferation, with cell density increasing by 5-6 fold in 7 d on all three constructs. Each value is mean ± sd; n = 5.

[4] Fluorescence of actin stress fibers inside the hUCMSCs adhering on the scaffolds. (A) Rigid CPC, (B) non-rigid CPC-microbead scaffold, and (C) non-rigid CPC-microbead-fiber scaffold. (D) Higher magnification showing examples of actin stress fibers. (E) Actin stress fiber fluorescence intensity (mean ± sd; n = 5). These three values are significantly different from each other ($p < 0.05$).

[5] SEM of hUCMSC attachment on scaffolds. (A) hUCMSC attachment on rigid CPC construct at 1 d. (B) and (C) hUCMSC anchorage and spreading on the non-rigid CPC-microbead-fiber construct. "C" refers to the hUCMSCs. Cells developed long cytoplasmic extensions "E" that anchored to the fibers "F". (D) Higher magnification of cell attaching to the nano-apatite crystals in CPC. hUCMSCs attained a normal polygonal morphology.

[6] hUCMSC osteogenic differentiation. (A) Alkaline phosphatase activity (ALP) gene expression. (B) Osteocalcin (OC) expression. (C) Collagen type I expression. ALP was minimal at 1 d, peaked at 4 d, then decreased at 8 d. OC and collagen I peaked at 8 d. hUCMSCs on non-rigid CPC-microbead-fiber construct had higher ALP, OC and collagen I expressions than those on conventional rigid CPC. Each value is mean ± sd; n = 5.

[7] Alizarin Red S (ARS) staining of bone mineralization. It stains calcium minerals into a red color. (A) hUCMSCs on TCPS in control media at 14 d. (B) hUCMSCs on TCPS in osteogenic media at 14 d. (C) CPC disk with no cells. (D) Rigid CPC, (E) non-rigid CPC-microbead scaffold, and (F) non-rigid CPC-microbead-fiber scaffold. D-F were seeded with hUCMSCs and cultured in osteogenic media for 14 d. (G) Mineral concentration measured via the osteogenesis assay (mean ± sd; n = 5). hUCMSCs synthesized more mineral on the non-rigid CPC-microbead-fiber scaffold than that of the other two constructs ($p < 0.05$).

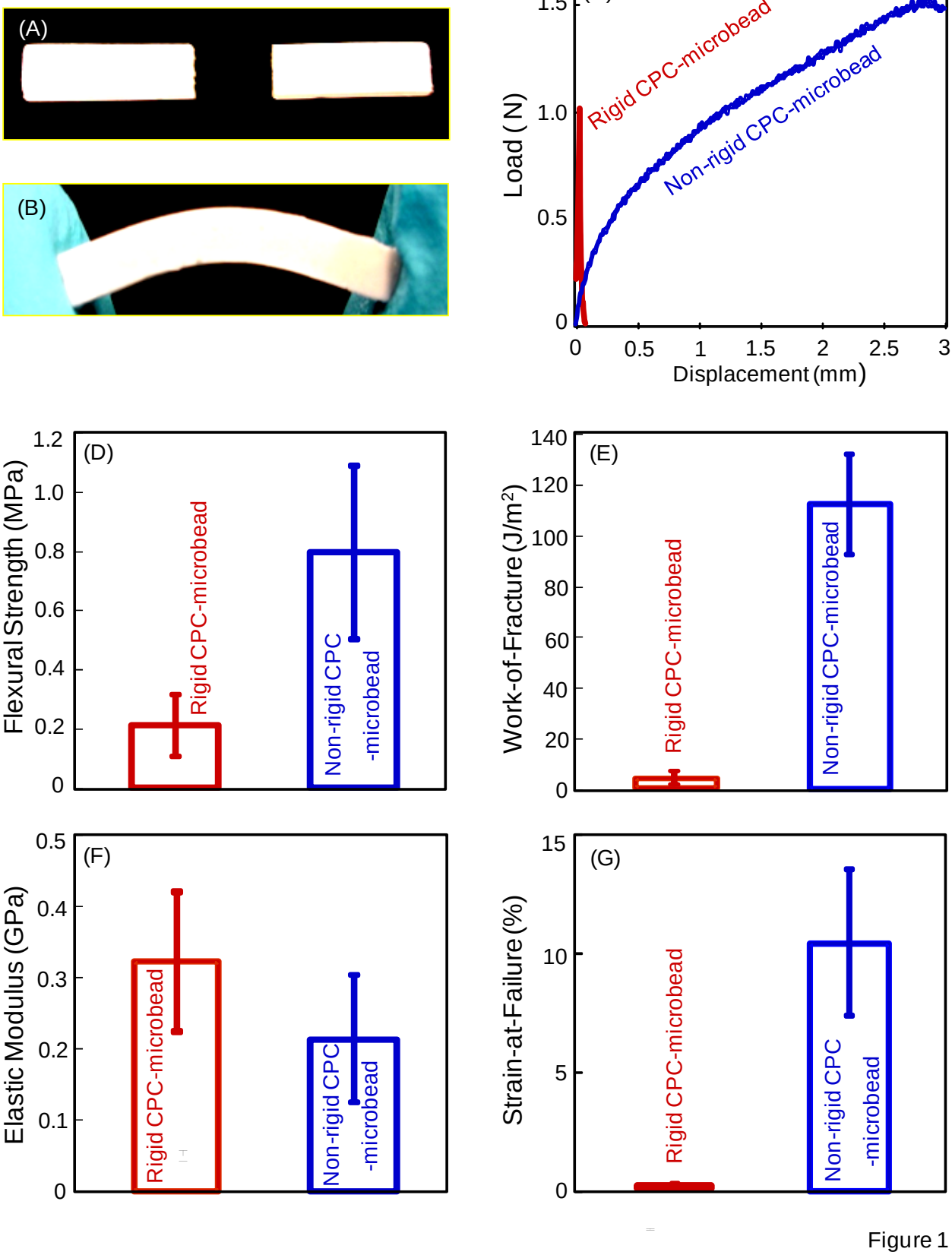
(A)
(B)
(C)
Load (N)
Displacement (mm)
Rigid CPC-microbead
Non-rigid CPC-microbead
(D)
Flexural Strength (MPa)
Rigid CPC-microbead
Non-rigid CPC -microbead
(E)
Work-of-Fracture (J/m²)
Rigid CPC-microbead
Non-rigid CPC-microbead
(F)
Elastic Modulus (GPa)
Rigid CPC-microbead
Non-rigid CPC -microbead
(G)
Strain-at-Failure (%)
Rigid CPC-microbead
Non-rigid CPC -microbead

Figure 1

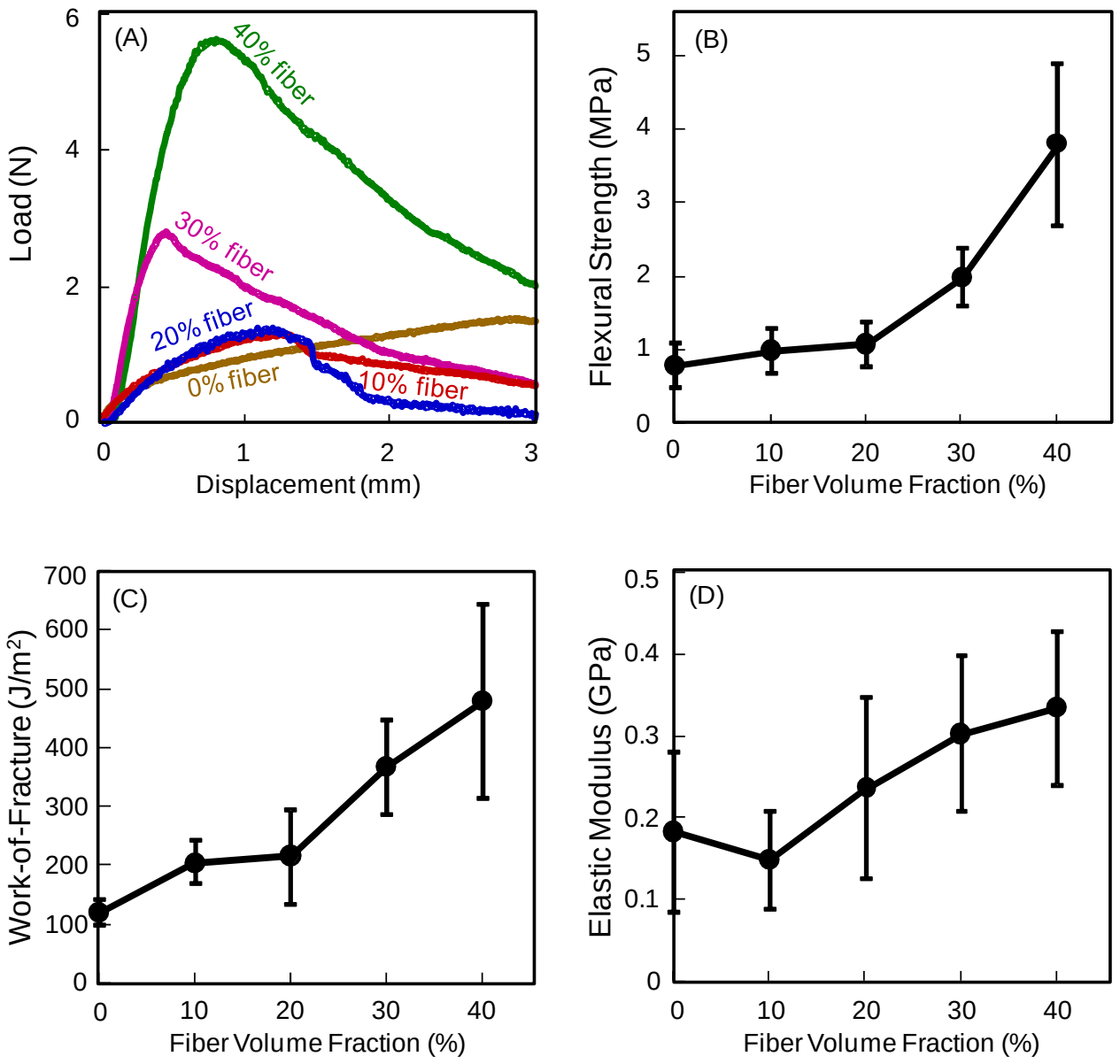
(A)
Load (N)
Displacement (mm)
40% fiber
30% fiber
20% fiber
10% fiber
0% fiber
(B)
Flexural Strength (MPa)
Fiber Volume Fraction (%)
(C)
Work-of-Fracture (J/m²)
Fiber Volume Fraction (%)
(D)
Elastic Modulus (GPa)
Fiber Volume Fraction (%)

Figure 2

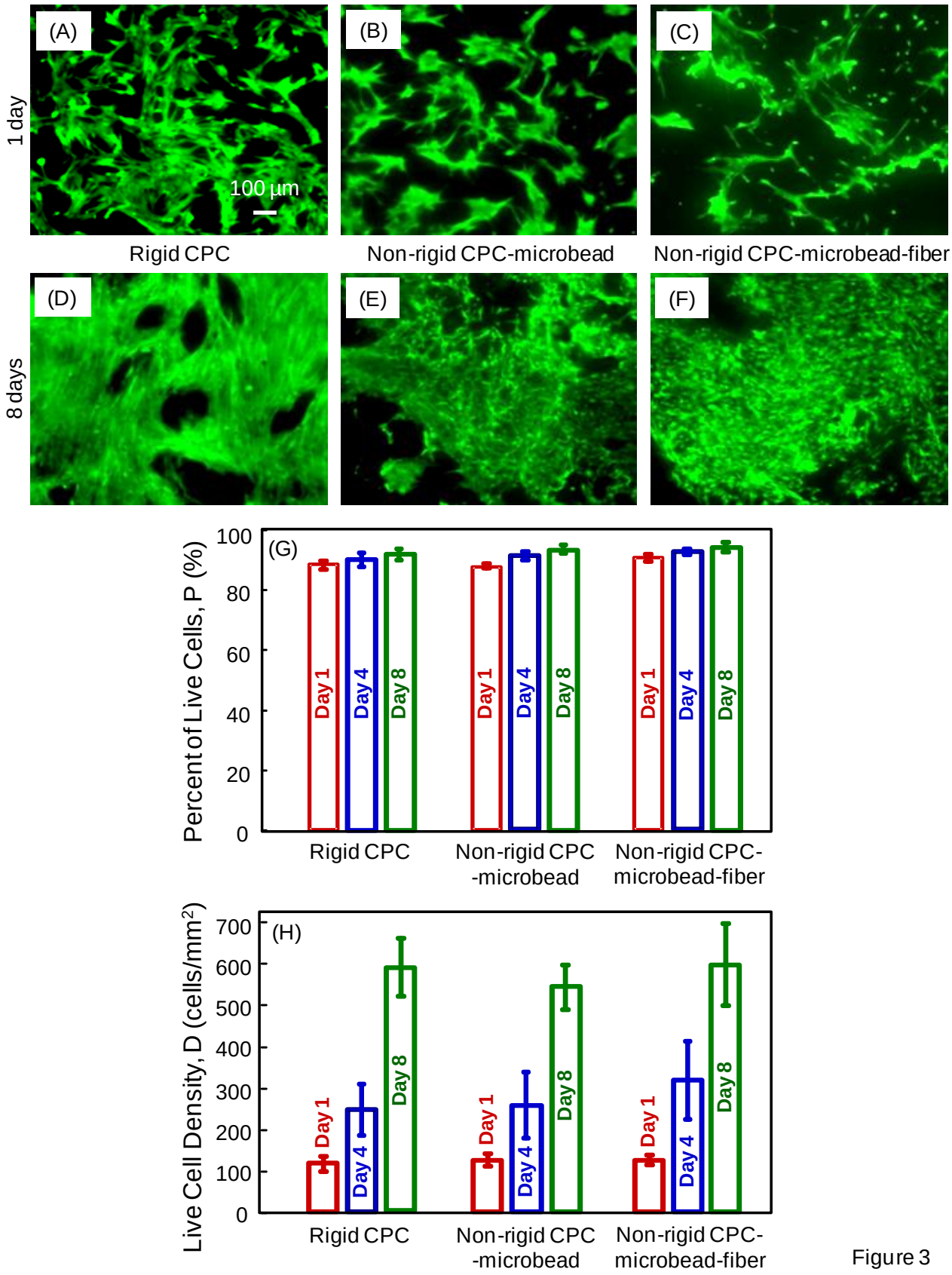
(A)
(B)
(C)
1 day
100 µm
Rigid CPC
Non-rigid CPC-microbead
Non-rigid CPC-microbead-fiber
(D)
(E)
(F)
8 days
(G)
Percent of Live Cells, P (%)
100
80
60
40
20
0
Day 1
Day 4
Day 8
Rigid CPC
Non-rigid CPC -microbead
Non-rigid CPC-microbead-fiber
(H)
Live Cell Density, D (cells/mm2)
700
600
500
400
300
200
100
0
Day 1
Day 4
Day 8
Rigid CPC
Non-rigid CPC -microbead
Non-rigid CPC-microbead-fiber

Figure 3

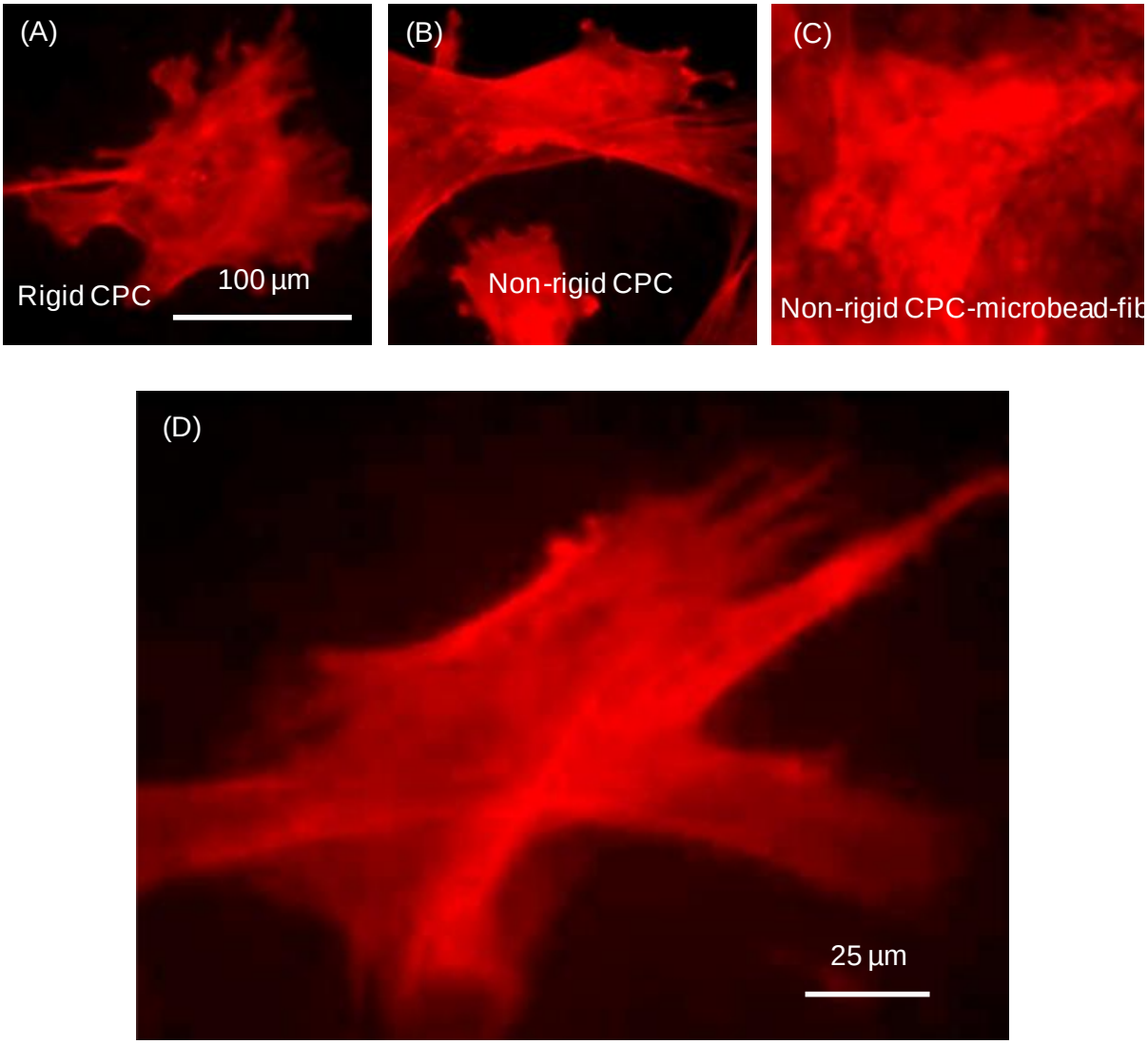
(A)
Rigid CPC
100 µm
(B)
Non-rigid CPC
(C)
Non-rigid CPC-microbead-fib
(D)
25 µm
(E)
hUCMSC Actin Stress Fiber
Fluorescence Intensity (arbitrary units)
15.0
12.5
10.0
7.5
5.0
2.5
0
Rigid CPC
Non-rigid CPC-microbead
Non-rigid CPC-microbead-fiber

Figure 4

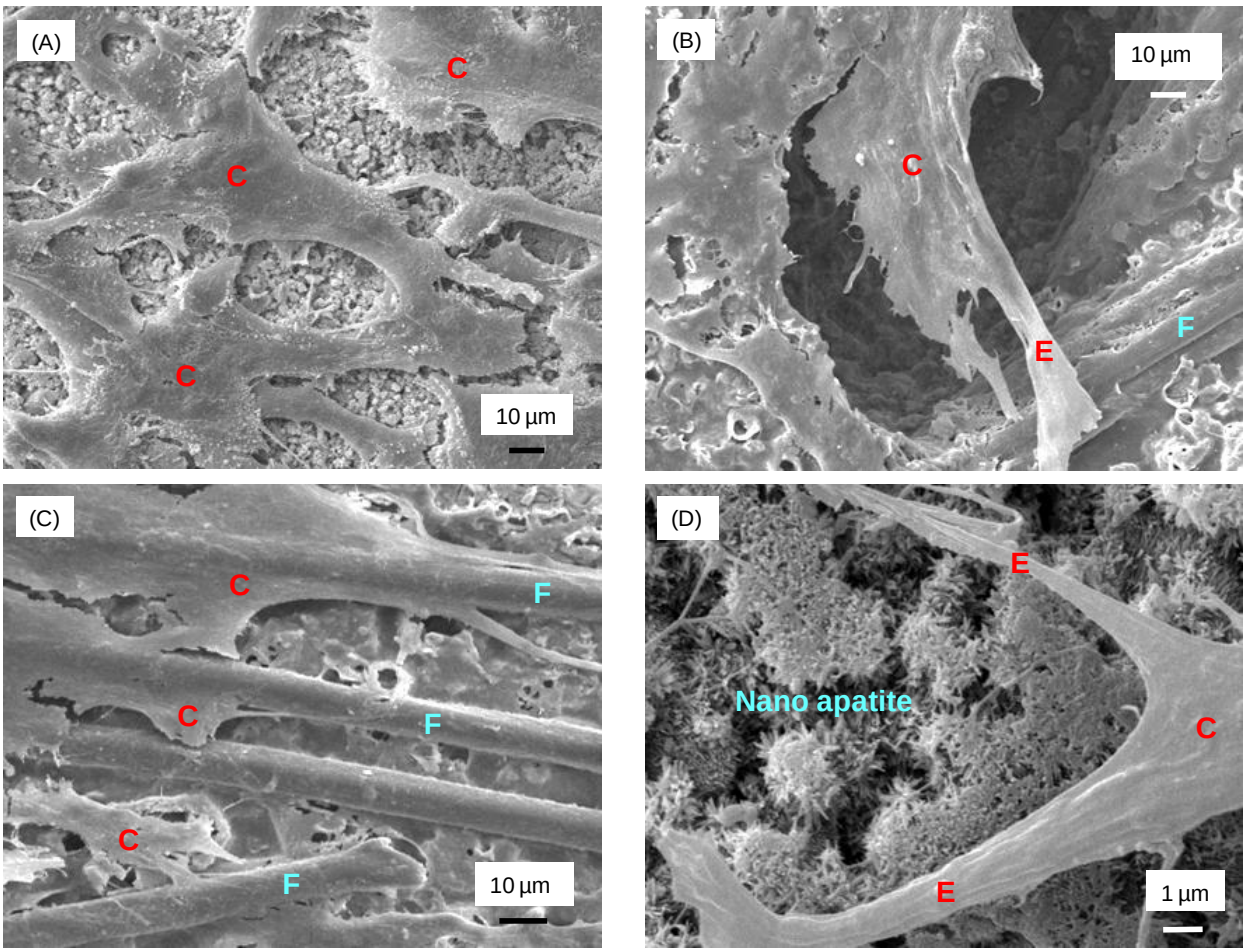

Figure 5

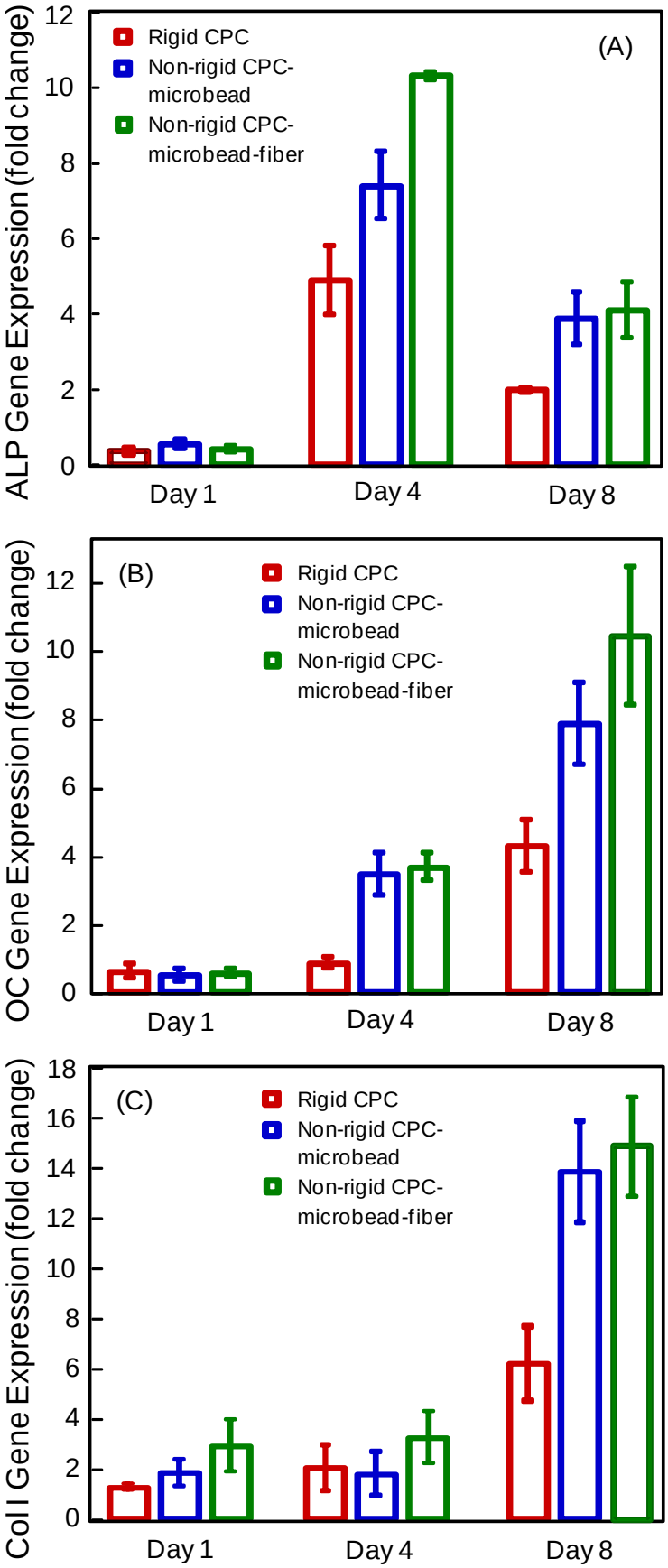
(A)
Rigid CPC
Non-rigid CPC-microbead
Non-rigid CPC-microbead-fiber
ALP Gene Expression (fold change)
0
2
4
6
8
10
12
Day 1
Day 4
Day 8
(B)
Rigid CPC
Non-rigid CPC-microbead
Non-rigid CPC-microbead-fiber
OC Gene Expression (fold change)
0
2
4
6
8
10
12
Day 1
Day 4
Day 8
(C)
Rigid CPC
Non-rigid CPC-microbead
Non-rigid CPC-microbead-fiber
Col I Gene Expression (fold change)
0
2
4
6
8
10
12
14
16
18
Day 1
Day 4
Day 8

Figure 6

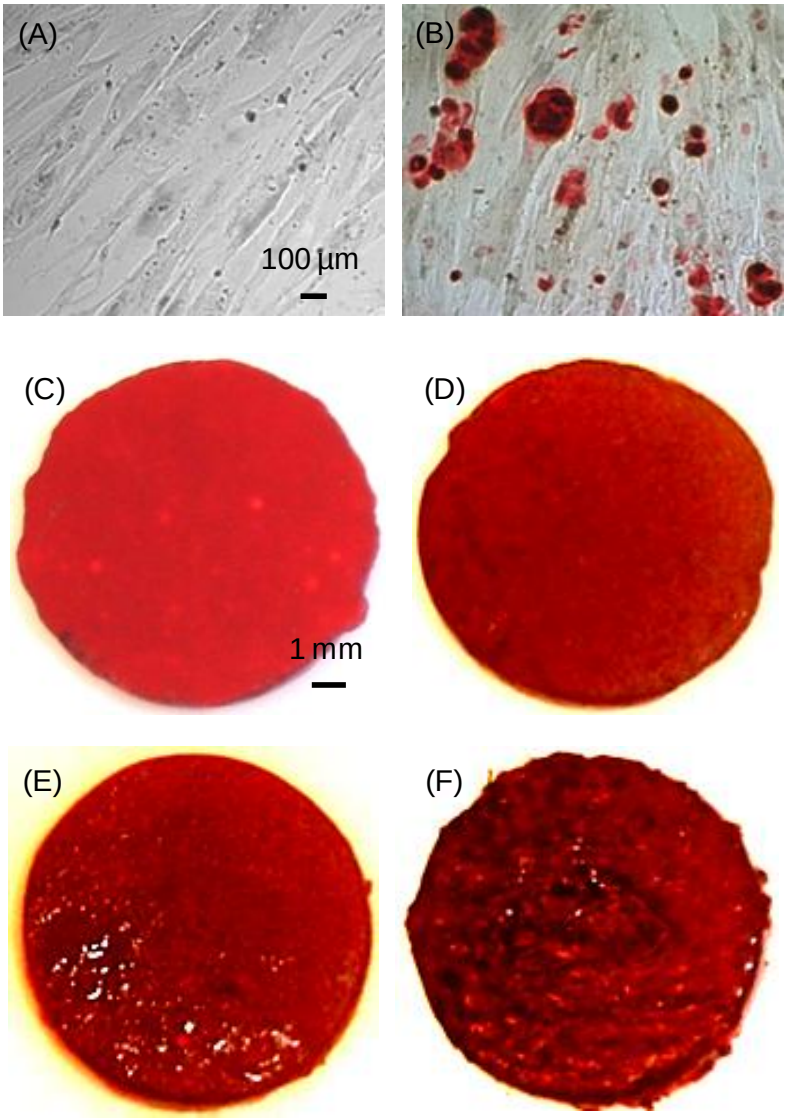
(A)
100 µm
(B)
(C)
1 mm
(D)
(E)
(F)
(G)
hUCMSC-Synthesized Mineral Concentration (mM)
0
0.5
1.0
1.5
Cells on rigid CPC
Cells on non-rigid CPC-microbead
Cells on non-rigid CPC-microbead-fiber

Figure 7